Quantification of volume, mass, and density of thrombus formation using brightfield and differential interference contrast microscopy

Sandra M. Baker-Groberg
Kevin G. Phillips
Owen J. T. McCarty

Quantification of volume, mass, and density of thrombus formation using brightfield and differential interference contrast microscopy

Sandra M. Baker-Groberg, Kevin G. Phillips, and Owen J. T. McCarty
Oregon Health and Science University, School of Medicine, Department of Biomedical Engineering, 3303 SW Bond Avenue, Portland, Oregon 97239

Abstract. Flow chamber assays, in which blood is perfused over surfaces of immobilized extracellular matrix proteins, are used to investigate the formation of platelet thrombi and aggregates under shear flow conditions. Elucidating the dynamic response of thrombi/aggregate formation to different coagulation pathway perturbations *in vitro* has been used to develop an understanding of normal and pathological cardiovascular states. Current microscopy techniques, such as differential interference contrast (DIC) or fluorescent confocal imaging, respectively, do not provide a simple, quantitative understanding of the basic physical features (volume, mass, and density) of platelet thrombi/aggregate structures. The use of two label-free imaging techniques applied, for the first time, to platelet aggregate and thrombus formation are introduced: noninterferometric quantitative phase microscopy, to determine mass, and Hilbert transform DIC microscopy, to perform volume measurements. Together these techniques enable a quantitative biophysical characterization of platelet aggregates and thrombi formed on three surfaces: fibrillar collagen, fibrillar collagen +0.1 nM tissue factor (TF), and fibrillar collagen +1 nM TF. It is demonstrated that label-free imaging techniques provide quantitative insight into the mechanisms by which thrombi and aggregates are formed in response to exposure to different combinations of procoagulant agonists under shear flow. © *2013 Society of Photo-Optical Instrumentation Engineers (SPIE)*. [DOI: 10.1117/1.JBO.18.1.016014]

1 Introduction

Recent work has demonstrated the ability to utilize commercially available imaging techniques to perform quantitative investigations of cellular mass, using low-numerical aperture (NA) illumination brightfield imagery,[1,2] and cellular volume,[3] using high NA illumination differential interference contrast (DIC) microscopy. Excitingly, these results demonstrate that key insights into the basic biophysical structure and composition of biological specimens are within reach using standard off-the-shelf optical microscopes employing label-free imaging modalities. To date, efforts to quantify the basic physical features of platelet thrombi and aggregates in the context of hemostasis and thrombosis have relied on fluorescent probes and confocal microscopy to quantify protein biodistribution and perform sample volume measurements using surface markers. While instructive, some of the limitations of confocal microscopy stem from the potential for nonspecific labeling by promiscuous antibodies and the lack of reagents or biomarkers for disease-specific applications. Moreover, confocal microscopy can provide only limited biophysical parameters—those dependent on the localization of the fluorescent label. DIC microscopy is commonly used to assess thrombi/aggregate surface area, but is limited to two-dimensional analyses of these complex structures.[4] To provide a three-dimensional and label-free biophysical picture of these structures, we have developed a label-free imaging strategy consisting of noninterferometric quantitative phase microscopy (NI-QPM)[5] and Hilbert transform DIC microscopy[6] to quantify the mass, volume, and density of platelet aggregates and thrombi formed *in vitro* using a flow chamber assay.[7] This platform is amenable to optical imaging to monitor both time-dependent and endpoint metrics associated with clot formation.

NI-QPM is carried out using standard brightfield imagery. Brightfield images of weak index contrast specimens, such as cells, appear semi-transparent due to the weak scattering and low absorption of the illuminating light. The amplitude of transmitted waves thus remains relatively unchanged during propagation through the sample. However, thickness and density fluctuations within the sample create phase lags in the transmitted waves. Under the paraxial approximation to the full wave dynamics, the phase of the transmitted waves can be related to the axial variation of the intensity of these waves via the transport of intensity equation. [5] To satisfy the assumptions of the paraxial approximation, low (NA = 0.1) transillumination combined with through-focus brightfield imaging form the basis of the input to the transport of intensity equation to perform phase measurements of the transmitted field through the sample. We have recently validated the NI-QPM method on polystyrene spheres ranging in size from 0.11 to 4.8 μm in diameter, which produce phase shifts ranging from 0.25 to 11 radians.[2] To determine mass, phase is then mapped to the axially integrated mass density of the specimen[8] to produce a projected mass density image. Summation of the area of the projected mass density image gives the total mass of the specimen.[9]

Address all correspondence to: Owen J. T. McCarty, Oregon Health and Science University, School of Medicine, Department of Biomedical Engineering, 3303 SW Bond Avenue, Portland, Oregon 97239. Tel: +503-418-9307; Fax: 503-418-9311; E-mail: mccartyo@ohsu.edu

Hilbert transform DIC (HT-DIC) microscopy, used to quantify specimen volume, can be performed on standard optical microscopes as well. The Hilbert transform is a spatial frequency space multiplier operator that creates symmetric image features through the maintenance of positive frequency components and the reversal of negative frequency components.[6] The utility of the transform lays in its ability to remove the bas relief of differential interference contrast (DIC) images, thus enabling the ability to threshold the background intensity values out of the image. This is not possible in DIC images as the gray levels of the specimen overlap the gray levels of the background. The ability to threshold the specimen away from the background comes with the artificial introduction of low frequency components which give rise to axial blurring.[10] The application of a high-pass Fourier filter eliminates this axial blurring to facilitate edge detection of specimens in DIC image cubes.[11] In a recent study, we have demonstrated that the HT-DIC method is equivalent to confocal fluorescence microscopy when determining geometric sample parameters, and is valid for samples above 0.11 μm in diameter.[4]

The combination of the NI-QPM method with the HT-DIC post processing procedure is a powerful image analysis combination that enables the determination of sample mass, volume, and density fluctuations in different regions of interest within a sample. In the current study, we utilize the NI-QPM—HT-DIC method to analyze the geometric parameters of platelet aggregates and thrombi formed under conditions of shear.

Collagen is a protein found in connective tissues, and when exposed to whole blood in circulation, such as in damaged endothelium, platelets bind to collagen via the adhesive protein von Willebrand factor (VWF).[12] The process of platelet recruitment, adhesion, activation and aggregate formation is termed primary hemostasis. Tissue factor (TF) is a protein expressed on the surface of subendothelial cells and when bound to coagulation factor VIIa, can activate factor X to initiate thrombin generation, resulting in fibrin formation.[13] As collagen-bound platelets become activated, they provide a surface for the activation of the coagulation cascade. This process of leads to local generation of fibrin on the growing platelet plug, termed thrombus formation or secondary hemostasis.

2 Materials and Methods

To investigate and characterize the physical parameters of platelet aggregation and thrombus formation, human whole blood was perfused over three different surfaces containing immobilized procoagulant agonists: fibrillar collagen, fibrillar collagen with relipidated human recombinant TF (Dade Innovin, Siemens Healthcare Diagnostics, Deerfield, Illinois) at a concentration of 0.1 nM, and fibrillar collagen with TF at 1 nM. Calcium ions present in whole blood are essential for the activation of coagulation factors. Experimental chelation of calcium ions in whole blood by the anticoagulant, sodium citrate, prevents the activation of coagulation factors, thus allowing for only platelet aggregation to occur. Recalcification of sodium citrate-anticoagulated whole blood with excess molar calcium and magnesium results in thrombin generation and thrombus formation.

Venous blood was collected from healthy volunteers into one-tenth sodium citrate (NaCit, 0.38% w/v).[14] Glass capillary vitrotubes (0.2 × 2.0 × 50 mm, Vitrotube™ Catalog # 5002, VitroCom, Mountain Lakes, New Jersey) were coated with fibrillar collagen (100 μg/mL, 1 h at 25°C), followed by washing with PBS. Collagen-coated slides were then either blocked with BSA (5 mg/mL, 1 h at 25°C) or coated with TF (1 h, at 25°C) at 0.1 or 1 nM, followed by washing with PBS and blocking with BSA. Coated vitrotubes were assembled onto microscope slides and mounted onto the stage of an inverted microscope (Zeiss Axiovert 200M, Carl Zeiss MicroImaging GmbH, Germany).[13] A pulse-free syringe pump perfused NaCit-anticoagulated blood through coated vitrotubes for 5 min at the physiologically relevant shear rate of 200 s^{-1} to form platelet aggregates. In order to form thrombi under shear, venous blood collected into one-tenth NaCit was mixed with calcium flow buffer (75 mmol/L CaCl$_2$ and 37.5 mmol/L MgCl$_2$) using a separate syringe pump prior to perfusion in order to trigger coagulation and drive fibrin formation.[13] Vitrotubes containing either platelet aggregates or thrombi were washed for 5 min with modified Hepes/Tyrode buffer (136 mmol/L NaCl, 2.7 mmol/L KCl, 10 mmol/L Hepes, 2 mmol/L MgCl$_2$, 2 mmol/L CaCl$_2$, 5.6 mmol/L glucose, 0.1% BSA; pH 7.45) at the same shear rate to remove unbound blood components.
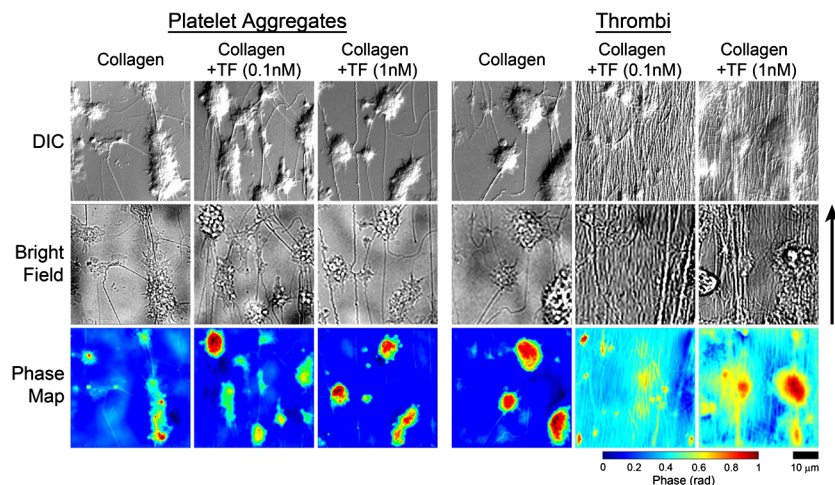

Fig. 1 Differential interference contrast (top row), brightfield (middle row), and corresponding NI-QPM phase map images (bottom row) for platelet aggregates and thrombi formed on three surfaces: fibrillar collagen, fibrillar collagen +0.1 nM TF, and fibrillar collagen +1 nM TF. The arrow indicates direction of flow. The scale and color bars are common to all images.

The samples were then fixed with paraformaldehyde (PFA, 4%) for image analysis.[15]

Through-focus, z-stack brightfield and DIC imaging from four random fields of view ($50 \times 50 \ \mu m^2$) of the samples were performed at $\times 63$ magnification with an oil-coupled, 1.4 NA objective lens on a Zeiss Axio Imager 2 microscope (Carl Zeiss MicroImaging GmbH, Germany). Three hundred through-focus transverse brightfield images were taken using an illumination condenser NA of 0.1 with a green filter ($\lambda = 540 \pm 20$ nm, Chroma Technology Corp., Bellows Falls, Vermont), while DIC images were taken with a condenser NA of 0.9. Images were taken at 0.1 μm axial increments. Z-stack images were taken from the surface of the slide to 5 μm above the platelet aggregate or thrombi, which ranged in height from 2 to 15 μm, in accord with previous studies (Fig. 1).[16] The microscope was operated under software control by SlideBook 5.5 (Intelligent Imaging Innovations, Denver, Colorada).
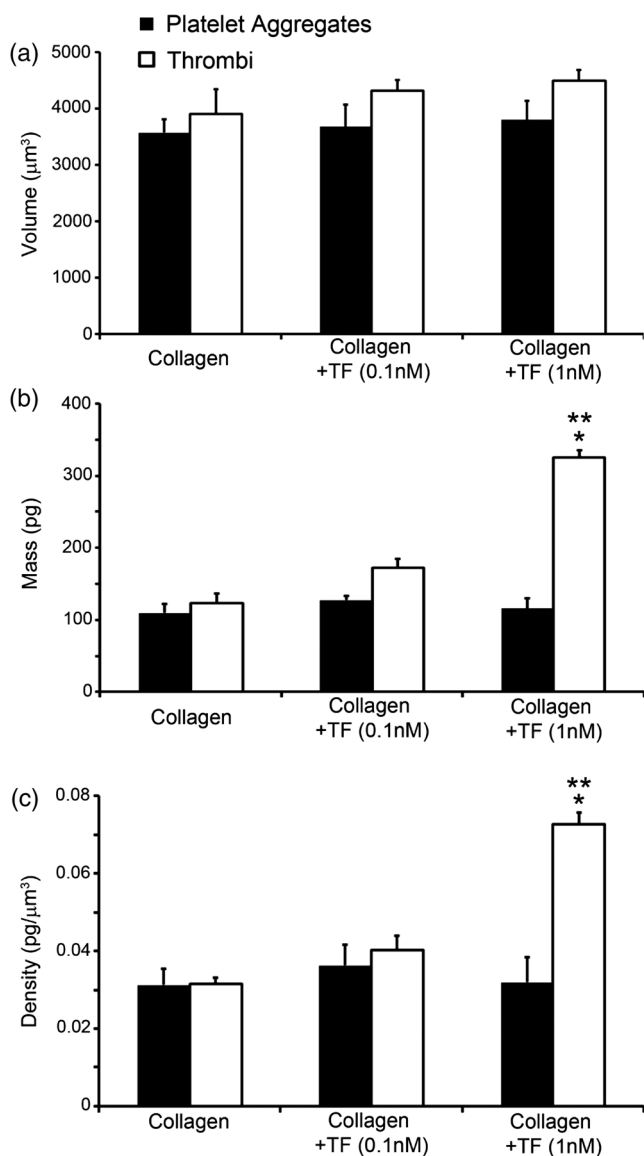

Fig. 2 (a) Mean volume, (b) mass, and (c) density of platelet aggregates and thrombi for a $50 \times 50 \ \mu m^2$ field of view. Error bars are $\pm$ SEM. $*$ denotes a p-value ≤ 0.01 in comparison to platelet aggregate values and $**$ indicates a p-value ≤ 0.01 compared with collagen-coated slides.

To obtain volume measurements [Fig. 2(a)], the cross-sectional planes of the HT-DIC images of the sample were detected using a Sobel-based edge detection with the area computed in each plane and then added together using a custom program written in MATLAB® (The MathWorks, Inc., USA).[3] Mass measurements [Fig. 2(b)] were taken using the NI-QPM technique, where measured intensity values were used to approximate the axial derivative of the intensity, followed by the application of a Green function technique to solve for phase numerically.[11,17] Lastly, projected sample mass density was determined using a custom MATLAB® program, followed by integration over the area of the sample to retrieve total sample mass.[2] Volume and mass calculations were used to calculate the mean density [Fig. 2(c)] of platelet aggregates and thrombi formed over the three surfaces.

3 Results and Discussion

Whole blood collected into NaCit resulted in only platelet-collagen adhesion and platelet-platelet aggregations (Fig. 1), while the addition of calcium and magnesium to NaCit-anticoagulated whole blood activated coagulation factors to form fibrin (Fig. 1) and create thrombi. Mean volume of platelet aggregates and thrombi did not significantly differ between the three surfaces [Fig. 2(a)], however; mean mass [Fig. 2(b)] and density [Fig. 2(c)] significantly increased from 122.8 ± 14.1 pg and 0.03 ± 0.002 pg/μm^3 to 325.0 ± 10.7 pg and 0.07 ± 0.003 pg/μm^3 (p-value ≤ 0.01) for thrombi formed on fibrillar collagen $+1$ nM TF compared with fibrillar collagen alone.

Evaluation of the physical features of thrombi and aggregates can be carried out using specific fluorescent probes imaged under confocal microscopy to quantify volume.[18] However, structural quantitative information, such as density, cannot be investigated with confocal microscopy. Two dimensional analysis of thrombi and aggregates imaged under DIC (Fig. 1) demonstrate TF-dependent fibrin formation in the presence of calcium and magnesium, though the quantification of the biophysical changes among thrombi is confined to area alone. These two dimensional images cannot reveal the three dimensional organization of platelet aggregates and fibrin formation. Interestingly, NI-QPM and HT-DIC revealed that although the volume of formed thrombi on a surface of collagen $+1$ nM TF was similar to the other treatments, the mass and density of the thrombi formed with 1 nM TF increased significantly, presumably due to an increased degree of fibrin formation for the same equivalent number of platelets. This parallels confocal-based observations of fluorescent fibrin reporters, which indicate the presence of TF increases the number of fibrin cross-links in thrombi.[19]

Our results demonstrate the effectiveness of label-free imaging modalities to measure the basic physical features of platelet aggregates and thrombi structures. Having the capability of determining clot density in a fast, accurate, and technologically accessible manner will provide investigators a quantitative means to characterize the efficacy of novel antithrombotics and treatment strategies to inhibit thrombus formation.

References

1. K. G. Phillips, S. L. Jacques, and O. J. T. McCarty, "Measurement of single cell refractive index, dry mass, volume, and density using a transillumination microscope," *Phys. Rev. Lett.* **109**(11), 118105 (2012).

2. K. G. Phillips et al., "Optical quantification of cellular mass, volume, and density of circulating tumor cells identified in an ovarian cancer patient," *Front. Oncol.* **2**(72), 1–8 (2012).

3. S. M. Baker, K. G. Phillips, and O. J. T. McCarty, "Development of a label-free imaging technique for the quantification of thrombus formation," *Cell. Mol. Bioeng.* **5**(4), 488–492 (2012).

4. J. E. Aslan et al., "S6K1 and mTOR regulate Rac1-driven platelet activation and aggregation," *Blood* **118**(11), 3129–3136 (2011).

5. D. Paganin and K. A. Nugent, "Non-interferometric phase imaging with partially coherent light," *Phys. Rev. Lett.* **80**(12), 2586–2589 (1998).

6. M. R. Arnison et al., "Using the Hilbert transform for 3D visualization of differential interference contrast microscope images," *J. Microsc.* **199**(1), 79–84 (2000).

7. O. J. McCarty et al., "Evaluation of platelet antagonists in *in-vitro* flow models of thrombosis," *Methods of Mol. Med.* **93**, 21–34 (2004).

8. R. Barer, "Interference microscopy and mass determination," *Nature* **169**(4296), 366–367 (1952).

9. G. Popescu, "Quantitative phase imaging of nanoscale cell structure and dynamics," in *Methods in Cell Biology*, B Jena, Ed., Vol. 90, PP. 87–115, Elsevier, Burlington (2008).

10. C. Preza et al., "Determination of direction-independent optical path-length distribution of cells using rotational-diversity transmitted-light differential interference contrast (DIC) images," *Proc. SPIE* **3261**, 60–70 (1998).

11. K. G. Phillips et al., "Quantification of cellular volume and sub-cellular density fluctuations: comparison of normal peripheral blood cells and circulating tumor cells identified in a breast cancer patient," *Front. Oncol.* **2**(96), 1–10 (2012).

12. O. J. T. McCarty et al., "von Willebrand factor mediates platelet spreading through glycoprotein Ib and alpha(IIb)beta3 in the presence of botrocetin and ristocetin, respectively," *J. Thromb. Haemost.* **4**(6), 1367–1378 (2006).

13. M. A. Berny et al., "Spatial distribution of factor Xa, thrombin, and fibrin(ogen) on thrombi at venous shear," *PLoS One* **5**(4), e10415 (2010).

14. T. C. White-Adams et al., "Laminin promotes coagulation and thrombus formation in a factor XII-dependent manner," *J. Thromb. Haemost.* **8**(6), 1295–1301 (2010).

15. T. C. White et al., "The leech product saratin is a potent inhibitor of platelet integrin alpha2beta1 and von Willebrand factor binding to collagen," *FEBS J.* **274**(6), 1481–1491 (2007).

16. O. J. T. McCarty et al., "Rac1 is essential for platelet lamellipodia formation and aggregate stability under flow," *J. Biol. Chem.* **280**(47), 39474–39484 (2005).

17. J. Frank, S. Altmeyer, and G. Wernicke, "Non-interferometric, non-iterative phase retrieval by green's functions," *J. Opt. Soc. Am. A Opt. Image Sci. Vis.* **27**(10), 2244–2251 (2010).

18. S. Falati et al., "Real-time *in vitro* imaging of platelets, tissue factor and fibrin during arterial thrombus formation in the mouse," *Nature Med.* **8**(10), 1175–1180 (2002).

19. R. A. Campbell et al., "Contributions of extravascular and intravascular cells to fibrin network formation, structure, and stability," *Blood* **114**(23), 4886–4896 (2009).